

Theory of two strongly interacting resonances in multiphoton ionization

Burke Ritchie

Sandia Laboratories, Albuquerque, New Mexico 87185

(Received 24 September 1979)

The author presents a theory for N -photon ionization in which two intermediate states can be in resonance with the ground state over a narrow range of photon frequencies. The theory is applied to the three-photon $6F$ resonance-state spin-orbit doublet in the four-photon ionization of Cs. The amplitude for the process is the sum of two components, each containing a complex line-shape function. In the limit of zero splitting, the previously studied isolated resonance result, in which the line shape is Lorentzian is recovered. For the splitting in Cs ($6F$), the absorption profile is studied as a function of the splitting parameters of the state, the $6S \rightarrow 6F$ three-photon Rabi rate, and the field-induced shift and width for the $6S \rightarrow 6F$ transition. This profile depends in a complicated way on the relative magnitudes of the shift and the spacing between the fine-structure levels.

INTRODUCTION AND THEORY

In a recent paper¹ (I) a theory was presented for resonant multiphoton ionization in which the infinities of perturbation theory, which occur at the $(N-1)$ -photon excitation energies of the target, were removed by solving an integral equation [Eq. (10a) of I with the last term on the right-hand side omitted]. This equation was solved approximately very near a resonance by representing the singular Green's function by the eigenfunction Ψ_I of the resonant intermediate state. This procedure yields an analytic result which was later² (II) identified with a limiting case of steady-state density-matrix theory.^{3,4} In II it was pointed out that the theory of I is valid for the inequality $\frac{1}{2}\Omega_I^2 \ll \frac{1}{4}(R_I)^2$, where Ω_I is the order $N-1$ Rabi rate for the ground- to intermediate-state transition and R_I is the intermediate-state one-photon ionization rate. These are (for $N \geq 2$)

$$\frac{1}{2}\Omega_I = \frac{\omega_p}{E_p} \left(\frac{2\pi F \alpha a_0^2}{\omega_p} \right)^{(N-1)/2} |\langle \Psi_I | \hat{\rho} \cdot \vec{\nabla} | \chi_{N-2} \rangle|, \quad (1a)$$

$$R_I = \frac{F \alpha a_0^2}{2\pi} \frac{k}{E_p} \int d\Omega |\langle \Psi_k^{(-)} | \hat{\rho} \cdot \vec{\nabla} | \Psi_I \rangle|^2, \quad (1b)$$

where F is the photon flux in $\text{cm}^{-2} \text{s}^{-1}$, ω_p is the photon frequency in s^{-1} corresponding to E_p atomic units of energy, α is the fine-structure constant, a_0 is the Bohr radius, k is the ejected-electron momentum in atomic units, Ω is the solid angle into which the electron is ejected, and $\hat{\rho}$ is the unit vector in the direction of polarization of the photon; Ψ_I , $\Psi_k^{(-)}$, and χ_{N-2} are, respectively, the intermediate-state, final continuum-state, and order $N-2$ perturbed-state wave functions. At fluxes corresponding to intensities of about 1 GW cm^{-2} , simple dimensional analysis of Eqs. (1) shows that the inequality above is likely to be

satisfied for $N \geq 4$. There are an increasing number of experiments being performed for such higher-order processes, and the result of I has been applied to the interpretation of data⁶ for the four-photon ionization of Cs near the $6F$ resonance.

It is the purpose of this paper to present the resonant N -photon ionization rate in which two intermediate states can be in resonance over a narrow range of frequencies. To account exactly for all states of the atomic spectrum would require the numerical solution of the integral equation of I. However, for two closely spaced levels the process is dominated by two eigenstates of this spectrum. A case of special interest is that in which the field-induced shifts and widths of the two transitions can be significant fractions of their spacing. This result is applied to the spin-orbit doublet of the Cs $6F$ level.⁷

When the singular Green's function is represented by two eigenfunctions Ψ_1 and Ψ_2 , the integral equation of I can still be solved analytically [see Eq. (14a) of I for the one-eigenfunction analytic solution]. When this solution is used to derive the rate [see Eq. (5) of II or Eq. (2a) of Ref. 5 for the isolated resonance rate], we obtain

$$R_N = R_1 |g_{12}(\delta_1, \delta_2)|^2 + R_2 |g_{21}(\delta_2, \delta_1)|^2 + 2 \text{Re} \int d\Omega [f_1 g_{12}(\delta_1, \delta_2)]^* f_2 g_{21}(\delta_2, \delta_1), \quad (2)$$

where R_1 and R_2 are the one-photon ionization rates for intermediate levels one and two [Eq. (1b) with I replaced by 1 or 2], corresponding to photoelectric amplitudes f_1 and f_2 , where $dR_j/d\Omega = F |f_j|^2$ [see Eq. (1b)]. The complex line-shape function is defined as

$$g_{ij}(\delta_i, \delta_j) = \frac{\frac{1}{2}[\Omega_i(1-f_{jj}) + \Omega_j f_{ij}]}{(\delta_i - \frac{1}{2}\Delta_{ii}^{(e)})(1-f_{jj}) - \frac{1}{2}\Delta_{ji}^{(e)} f_{ij}}, \quad (3)$$

where Ω_i and Ω_j are order $N-1$ Rabi rates [see Eq. (1a) with I replaced by i or j]. The static detuning from level i or j is δ_i or δ_j . For example,

$$\delta_j = (\omega_0 - \omega_j) + (N-1)\omega_p, \quad (4)$$

where ω_0 and ω_j are the ground and j th intermediate-state eigenfrequencies. The quantity f_{ij} is the ratio of a complex shift function $\frac{1}{2}\Delta_{ij}^{(c)}$ to the static detuning δ_j or $f_{ij} = \frac{1}{2}\Delta_{ij}^{(c)}/\delta_j$. This complex shift^{1,2} is defined by

$$\Delta_{ij}^{(c)} = \frac{-8\pi F \alpha a_0^2}{E_p} \sum_{n=N-2}^N \iint d\vec{r} d\vec{r}' \Psi_i^*(\vec{r}) (\hat{\rho} \cdot \vec{\nabla}) \times g^{(M)}(\vec{r}, \vec{r}', 2(E_0 + nE_p)) (\hat{\rho} \cdot \vec{\nabla}') \Psi_j(\vec{r}'), \quad (5)$$

where $g^{(M)}$ is the Green's function appropriate for the atomic field, E_0 is the ground-level energy in atomic units, and the prime on the summation means that the $n=N-1$ term is omitted as parity nonconserving (i and j are assumed to be states having the same orbital angular momentum, and the parity of n - and the l -wave components of $g^{(M)}$ must be the same). The field-induced level shifts and widths are proportional to the real and imaginary parts of the diagonal elements of the $\Delta^{(c)}$ matrix, respectively. Note that the diagonal and nondiagonal elements of $\Delta^{(c)}$ are closely related to the Rayleigh and Raman scattering amplitudes, respectively, for states i and j [for example, see Eq. (A6) of II where, on resonance, we relate a diagonal element of $\Delta^{(c)}$ to the frequency-dependent polarizability of the intermediate state]. The calculation of atomic parameters is described in the Appendix.

For linearly polarized light only the $M_J = \pm \frac{1}{2}$ sublevels of the $J = \frac{7}{2}$ or $J = \frac{5}{2}$ components of the $6F$ state are accessible from the ground $J = \frac{1}{2}$, $M_J = \pm \frac{1}{2}$ levels. In this case Eq. (3) takes a particularly simple form,

$$g_{ij}(\delta_i, \delta_j) = \frac{1}{2} c_i^2 \Omega_3 / [\delta_i - \Delta^{(c)} (c_i^2 + \delta_i \delta_j^{-1} c_j^2)], \quad (6a)$$

$$\Delta^{(c)} = \Delta + \frac{1}{2} i R_{6F}, \quad (6b)$$

where, for LS states, Ω_3 (Table I) is the three-photon Rabi rate and $\Delta^{(c)}$ (Table I) [Eq. (5) times $\frac{1}{2}$ for $i=j=6F$] is the complex shift for the $6S \rightarrow 6F$ transition. The constants c_i and c_j are the Clebsch-Gordan coefficients for the coupling of the $l=3$ and $s=\frac{1}{2}$ states to give the i th (lower) state, $|\frac{5}{2}, \frac{1}{2}\rangle$, and j th (upper) state, $|\frac{7}{2}, \frac{1}{2}\rangle$, respectively. These are

$$c_i = \langle 30 \frac{1}{2} \frac{1}{2} | \frac{5}{2} \frac{1}{2} \rangle = -\sqrt{\frac{3}{7}}, \quad (7a)$$

$$c_j = \langle 30 \frac{1}{2} \frac{1}{2} | \frac{7}{2} \frac{1}{2} \rangle = 2/\sqrt{7}; \quad (7b)$$

note that $c_i^2 + c_j^2 = 1$. Thus, when $\delta_i = \delta_j = \delta$ (zero splitting), the previously studied^{1,2,5} isolated resonance result is recovered,

TABLE I. Atomic parameters in units of frequency ω ($\omega/2\pi = c/\lambda$) at an intensity of 10^9 W cm⁻² or $F = 0.5335 \times 10^{28}$ cm⁻² s⁻¹ at $\delta = 0$ s⁻¹, where δ [see Eqs. (4) and (8)] is zero for a three-photon excitation energy of 3.51 eV.

	This work ^a
Ω_3	$= 1.735 \times 10^9$ s ⁻¹
R_{6F}	$= 1.569 \times 10^{10}$ s ⁻¹
Δ	$= 2.767 \times 10^{11}$ s ⁻¹
$\sigma_{6F}^{(V)}$	$= R_{6F}/F = 2.942 \times 10^{-18}$ cm ²
$\sigma_{6F}^{(L)}$	$= 2.720 \times 10^{-18}$ cm ²

^a The $6F$ -level photoelectric cross sections have been calculated independently by Pindzola (unpublished) using an iterative solution of the Hartree-Fock (static-exchange) equations for the e, Cs^+ system. These are found to be $\sigma_{6F}^{(V)} = 2.94 \times 10^{-18}$ cm² and $\sigma_{6F}^{(L)} = 2.92 \times 10^{-18}$ cm². My static results are $\sigma_{6F}^{(V)} = 2.578 \times 10^{-18}$ cm² and $\sigma_{6F}^{(L)} = 2.458 \times 10^{-18}$ cm². Thus exchange has a fairly small effect on this cross section at this energy ($\hbar^2 = 0.0579$ Ry) because it is dominated by the $6F \rightarrow kg$ transition. The $6F \rightarrow kd$ radial dipole amplitude is about a factor of two larger with exchange but is still much smaller than the $6F \rightarrow kg$ radial dipole amplitude, on which exchange has a negligible effect because of the large centrifugal barrier in the g -wave equation. Also, polarization forces could be expected to be relatively unimportant in this cross section for this reason. Finally, enforced orthogonality of the continuum waves to the occupied bound orbitals of the neutral has been found to be negligible for this cross section. Note that the above parameters have been calculated only at $\delta = 0$ s⁻¹; thus they have been assumed to be constant in energy over the range of values of δ displayed in the figures.

$$g_{12}(\delta) + g_{21}(\delta) = \frac{1}{2} \Omega_3 / (\delta - \Delta^{(c)}). \quad (8)$$

The same result for $g_{ij}(\delta_i, \delta_j)$ [Eq. (6)] obtains for $M_J = -\frac{1}{2}$ states; thus there is no spin polarization (Fano effect⁸) for linearly polarized photons, as is well known. In deriving Eq. (6) from Eqs. (2), (3), and (5), Ψ_i and Ψ_j of R_i and R_j [Eq. (2)], of Ω_i and Ω_j [Eq. (3)], and of $\Delta_{ij}^{(c)}$ [Eq. (5)] have been defined as the $J = \frac{5}{2}$, $M_J = \frac{1}{2}$ and $J = \frac{7}{2}$, $M_J = \frac{1}{2}$ states, respectively, using c_i and c_j [Eqs. (7)], and Hartree-Fock LS states (Appendix). There is cancellation of certain terms in the numerators and denominators of $f_1 g_{12}$ and $f_2 g_{21}$ leading to the simplified line-shape functions given by Eq. (6).

RESULTS AND DISCUSSION

The position of an isolated resonance [see Eq. (8)] occurs when $\delta = \Delta$. From Eq. (6a) the resonance positions for the doublet occur at the points

$$\delta_1 = \begin{cases} \frac{1}{2} \{ (\delta_s + \Delta) - [(\delta_s + \Delta)^2 - 4\delta_s \Delta c_1^2]^{1/2} \} & (9a) \\ \frac{1}{2} \{ -(\delta_s - \Delta) + [(\delta_s - \Delta)^2 + 4\delta_s \Delta c_2^2]^{1/2} \} + \delta_s, & (9b) \end{cases}$$

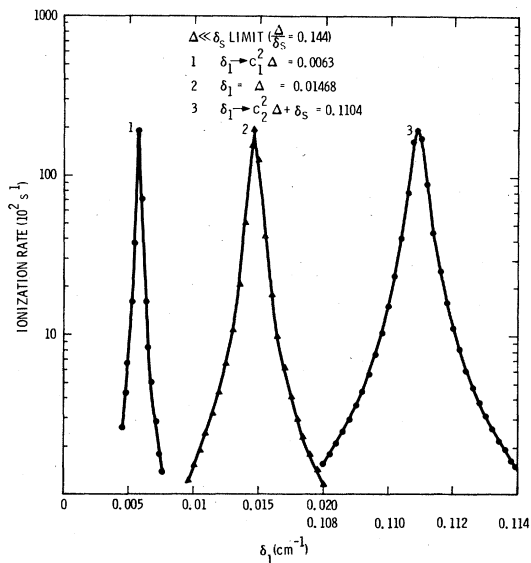


FIG. 1. Ionization rates vs detuning δ_1 from the first intermediate level for a laser intensity of 10^7 W cm^{-2} , where the shift Δ is much less than the fine-structure spacing δ_s ; c_1 and c_2 are the Clebsch-Gordan coefficients defined in the text. Curves 1 and 3 are for the spin-orbit doublet; curve 2 is for an isolated resonance (no spin-orbit splitting).

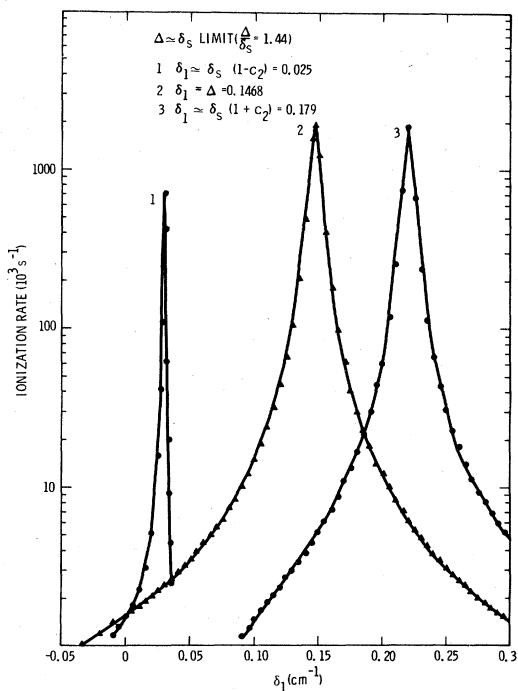


FIG. 2. Ionization rates vs detuning δ_1 from the first intermediate level for a laser intensity of 10^8 W cm^{-2} , where the shift Δ is nearly equal to the fine-structure spacing δ_s ; c_1 and c_2 are the Clebsch-Gordan coefficients defined in the text. Curves 1, 2, and 3 are defined in Fig. 1.

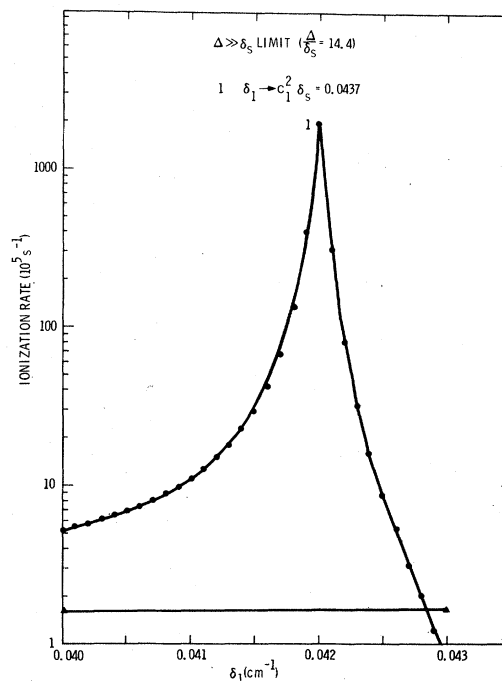


FIG. 3. Ionization rates vs detuning δ_1 from the first intermediate level for a laser intensity of 10^9 W cm^{-2} , where the shift Δ is much larger than the fine-structure spacing δ_s ; c_1 is a Clebsch-Gordan coefficient defined in the text. Curve 1 is defined as in Fig. 1. The lower curve Δ is curve 2, defined as in Fig. 1.

where δ_s is the spacing between the levels ($\delta_s = 0.102 \text{ cm}^{-1}$ for the $6F$ doublet) and, from Table I, $\Delta = 1.468 \text{ cm}^{-1}$ at 1 GW cm^{-2} . In Figs. 1–4 we study the ionization for three cases [see Eqs. (9)]: (i)

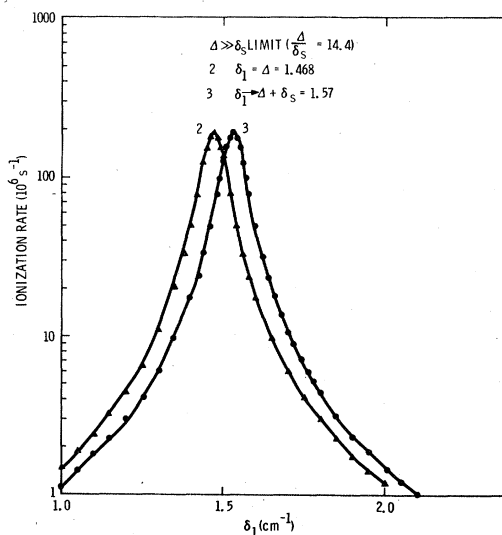


FIG. 4. See Fig. 3 caption. Curves 2 and 3 are defined as in Fig. 1.

$\delta_s \gg \Delta$, at an intensity of 0.01 GW cm^{-2} , for which $\delta_1 \approx c_1^2 \Delta$ and $\delta_1 \approx c_2^2 \Delta + \delta_s$; (ii) $\delta_s \approx \Delta$, at an intensity of 0.1 GW cm^{-2} , for which $\delta_1 \approx \delta_s(1 - c_2)$ and $\delta_1 \approx \delta_s(1 + c_2)$; and (iii) $\delta_s \ll \Delta$, at an intensity of 1 GW cm^{-2} , for which $\delta_1 \approx c_2^2 \delta_s$ and $\delta_1 \approx \Delta + \delta_s$. We use the parameters of Table I, the calculation of which is described in the Appendix, for all three cases. For cases (i) and (ii) we simply scale Δ and R_{eF} (proportional to F) by the factors 10^{-2} and 10^{-1} and Ω_s (proportional to $F^{3/2}$) the factors 10^{-3} and $10^{-3/2}$, respectively.

Note that in general the positions of the resonances (points of maximum ionization) have a quite complicated dependence on the relative magnitudes of the shift and doublet spacing. The limiting cases [(i) and (iii)] show a fairly simple dependence on δ_s and Δ . In (i) ($\delta_s \gg \Delta$) the two lines behave like the isolated resonance lines (in the center), but with their resonance positions δ_1 and δ_2 equal to $c_1^2 \Delta$ and $c_1^2 \Delta$ and $c_2^2 \Delta$, respectively (where $\delta_1 = \delta_2 + \delta_s$). In (iii) ($\delta_s \ll \Delta$) one line loses its dependence on the shift ($\delta_1 \approx c_2^2 \delta_s$), while the other ($\delta_1 \approx \Delta + \delta_s$) approaches Δ , the isolated resonance position. It is hoped that this study will stimulate further narrow-bandwidth experiments in which the absorption profile is studied as a function of the shift Δ relative to the fine-structure spacing δ_s .

ACKNOWLEDGMENTS

I wish to thank M. E. Riley for helpful discussion and M. S. Pindzola for supplying the atomic eigenfunctions used in this calculation. This work was supported by the U. S. Department of Energy.

APPENDIX

In this Appendix the calculation of the wave functions needed to evaluate the atomic parameters given by Eqs. (1) and (5) is described. All atomic orbitals are calculated in the Hartree-Fock approximation,⁹ with excited orbitals being calculated in the field of the ion; $R_f = R_{eF}$ [Eq. (1b)] is the imaginary part of Eq. (5) [see Eq. (A1b)] below. All energies are the experimental energies from

the tables of Moore.¹⁰ Orthogonalization of the ejected electron d wave to the occupied d orbitals of Cs was found to be negligible, as was the deviation from orthonormality of the Cs^+ and Cs orbitals.

The atomic-field Green's functions $g^{(M)}$ are calculated explicitly for energies nE above the ionization continuum ($n=4$) by using

$$g^{(M)} = (4\pi)^{-1} \times \sum_l (2l+1) g_l^{(M)}(r, r'; 2(E_{6s} + 4E_p)) P_l(\hat{\mathbf{r}} \cdot \hat{\mathbf{r}}'), \quad (\text{A1a})$$

$$g_l^{(M)} = -\frac{1}{kr r'} \times [G_l^{(M)}(kr_s) F_l^{(M)}(kr_c) + i F_l^{(M)}(kr) F_l^{(M)}(kr')], \quad (\text{A1b})$$

and by numerical solution for the regular and irregular waves $F_l^{(M)}$ and $G_l^{(M)}$, respectively, in an effective atomic field V (the static potential plus the semiclassical local exchange potential¹¹ appropriate for Cs^+). For energies nE below the ionization continuum ($n=2$) $g^{(m)}$ is found by defining the function

$$\chi_2^{(M)}(\vec{\mathbf{r}}) = \int d\vec{\mathbf{r}}' g^{(M)}(\vec{\mathbf{r}}, \vec{\mathbf{r}}'; 2(E_{6s} + 2E_p)) 2(\hat{\rho} \cdot \vec{\nabla}') \Psi_{6F}(\vec{\mathbf{r}}'), \quad (\text{A2})$$

which obeys the differential equation

$$[\nabla^2 - U(r) + 2(E_{6s} + 2E_p)] \chi_2^{(M)}(\vec{\mathbf{r}}) = 2\hat{\rho} \cdot \vec{\nabla} \psi_{6F}(\vec{\mathbf{r}}), \quad (\text{A3})$$

where $U = (2m_e/\hbar^2)V$. Here χ_2 [Eq. (1a) above] is the second-order perturbative response of the $6S$ state, and is calculated from the equation

$$[\nabla^2 - U(r) + 2(E_{6s} + 2E_p)] \chi_2(\vec{\mathbf{r}}) = 2\hat{\rho} \cdot \vec{\nabla} \chi_1(\vec{\mathbf{r}}); \quad (\text{A4})$$

χ_1 , the first-order perturbative response, is calculated from the equation

$$[\nabla^2 - U(r) + 2(E_{6s} + E_p)] \chi_1(\vec{\mathbf{r}}) = 2\hat{\rho} \cdot \vec{\nabla} \psi_{6s}(\vec{\mathbf{r}}). \quad (\text{A5})$$

The radial parts of Eqs. (A3)–(A5) are integrated numerically.

¹B. Ritchie, Phys. Rev. A **17**, 659 (1978).

²B. Ritchie, Phys. Rev. A **20**, 1734 (1979).

³J. L. F. de Meijere and J. H. Eberly, Phys. Rev. A **17**, 1416 (1978).

⁴J. H. Eberly and S. V. O'Neil, Phys. Rev. A **19**, 1161 (1979).

⁵B. Ritchie, Phys. Rev. Lett. **43**, 1380 (1979).

⁶J. Morellec, D. Normand, and G. Petite, Phys. Rev. A **14**, 300 (1976).

⁷G. Petite, J. Morellec, and D. Normand, J. Phys. (Paris) **40**, 115 (1979). The spin-orbit doublet of the $6F$ shift has been resolved in the experiment described

in this paper. A comparison between theory and experiment, however, would require treatment in the theory of the space-time distribution of the laser pulse, as in Ref. 5, for example.

⁸U. Fano, Phys. Rev. **178**, 131 (1969); **184**, 250 (1969).

⁹C. Froese, Phys. Rev. **4**, 1417 (1966); C. Froese Fisher, Comput. Phys. Commun. **1**, 151 (1969).

¹⁰C. E. Moore, Natl. Bur. Stand. (U.S.) Circ. No. 467 (U.S. GPO, Washington, D.C. 1949).

¹¹M. E. Riley and D. G. Truhlar, J. Chem. Phys. **63**, 2182 (1975).